Extended Brownian dynamics approach to diffusion-controlled processes

Gene Lamm[a] and Klaus Schulten[a]

Max-Planck-Institut für Biophysikalische Chemie, Göttingen, Federal Republic of Germany
(Received 12 September 1980; accepted 11 November 1980)

The method of Brownian dynamics to simultate trajectories of particles diffusing under the influence of external forces is extended to the approximation of local *linear* forces and to reflective boundaries possibly confining the diffusion space. A simple algorithm for the generation of random diffusive displacements is developed and its validity demonstrated by comparison with analytical and numerical descriptions of sample one-dimensional diffusion distributions.

I. INTRODUCTION

Reaction processes in the chemistry of dense media are to a large degree stochastic in nature and their theory has been the realm of statistical mechanics. The advent of experimental techniques to probe reaction processes on the nanosecond to picosecond time scale have borne out the realization that, even at such short times, reactions are often governed by diffusionlike motion. Recent examples include geminate recombination processes in liquids,[1] (photo) isomerization involving the motion of large molecular subunits,[2] polymer folding[3] and, particularly relevant in biochemistry, side group motion in proteins.[4] The Brownian character of these processes can be understood if one considers the time scale involved. For example, for geminate processes in the "solvent cage", i.e., reactions of two solutes after encounter, the reaction process involving many reencounters extends typically over a time much longer than the time τ_c of collisions with the bath and the momentum relaxation time τ_M of the solute. Consequently, a description of geminate recombination and many other processes can regard the motion of the reacting particles as Brownian.

Brownian motion involves to some degree hydrodynamic interactions between different particles (or molecular groups). These interactions can be taken into account (see, for example, Ref. 5). We will adopt here the common approximation which neglects hydrodynamic effects. However, even in the approximation of independent particle diffusion, theoretical descriptions of diffusion-controlled processes are generally limited to problems involving a high degree of (artificial) symmetry. The reason is that the Einstein-Smoluchowski diffusion equation basic to the description can be solved numerically essentially only for diffusion which can be reduced to one-dimensional motion, e.g., to the distance between two spherically symmetric particles. To overcome this limitation Schulten and Epstein[6] followed a suggestion by Ermak[7] and applied the method of Brownian dynamics. This method simulates large ensembles of diffusion trajectories corresponding to a certain process. The simulation is based on the algorithm to choose diffusive displacements during the time steps $\Delta t > \tau_M$ in accord with the Einstein-Smoluchowski diffusion equation. The close relationship of this method to the Wiener path integral formulation has been mentioned in Ref. 6.

The Brownian dynamics method developed so far is restricted in its range of application by the requirement of nearly *constant* local forces during random diffusive displacements covering time periods Δt. In this paper we provide an algorithm for random displacements which holds for (approximately) local linear forces. The algorithm requires little additional computational effort over the algorithm of Ermak but, because of its closer fit to an actual force field governing a diffusion process, should allow longer time steps Δt to be taken.

In many applications of the theory of diffusion-controlled processes the diffusion space is limited by boundaries; the physical origin of these boundaries is strong repulsive forces. The magnitude of these forces and their sudden onset represents a serious problem for any theory based on simple polynomial approximations of the force field. In the context of the diffusion equation, boundaries are traditionally cast into a boundary condition requiring the flux to vanish along the direction normal to the boundaries. In the following we also suggest an algorithm for random displacements which correctly simulates diffusion distributions near boundaries. We expect that the extended algorithm presented here increases the range of the method of Brownian dynamics to include many diffusion-controlled reaction processes of current interest.

II. A NEW ALGORITHM FOR DIFFUSIVE DISPLACEMENTS

We obtain an algorithm for simulating Brownian motion near a reflective boundary by considering the analytical result for the probability distribution in a constant force.[8] In this case the one-dimensional Einstein-Smoluchowski diffusion equation is

$$\frac{\partial}{\partial t}\, p(x,t|x_0) = \left(\frac{\partial^2}{\partial x^2} + b\,\frac{\partial}{\partial x}\right) p(x,t|x_0)\,, \tag{1}$$

where b is related to the force F by

$$b = -\beta F \tag{2}$$

and $\beta = 1/kT$, $t = D\times$time, D representing the diffusion constant. The solution of Eq. (1) is required to satisfy the initial condition

[a]New address: Department of Physics, Technical University of Munich, 8046 Garching bei München, FRG.

 0021-9606/81/130365-07$01.00

$$p(x, t=0|x_0) = \delta(x - x_0) , \tag{3}$$

as well as the reflective boundary condition

$$\frac{\partial}{\partial x} p(x, t|x_0) + b\, p(x, t|x_0) = 0 \quad \text{at } x = 0 . \tag{4}$$

The solution to Eqs. (1)–(4) may be written[8]

$$p(x, t|x_0) = \sum_{i=0,1,2} p_i(x, t|x_0) , \tag{5}$$

where

$$p_0(x, t|x_0) = (4\pi t)^{-1/2} \exp[-(x - x_0 + bt)^2/4t] , \tag{6}$$

$$p_1(x, t|x_0) = (4\pi t)^{-1/2} \exp[-bx_0 - (x + x_0 + bt)^2/4t] , \tag{7}$$

$$p_2(x, t|x_0) = \tfrac{1}{2} b \exp(-bx) \operatorname{erfc}[(x + x_0 - bt)/\sqrt{4t}] , \tag{8}$$

and $\operatorname{erfc}(z)$ denotes the complementary error function.[9] $p_0(x, t|x_0)$ describes the diffusion process in the absence of the boundary, i.e., solves Eqs. (1) and (3); the remaining terms account for the presence of the boundary. Our aim in this section is to develop an algorithm for random displacements which closely reproduces distribution (5) and to generalize the algorithm to linear forces near a boundary. The accuracy of the algorithm will be tested in Sec. III.

The relative probability that at time t the particles are distributed according to one of the three distributions (6), (7), or (8) is

$$N_i(t|x_0) = \int_0^\infty dx\, p_i(x, t|x_0), \quad i = 0, 1, 2 . \tag{9}$$

These integrals are found to be

$$N_0(t|x_0) = 1 - \tfrac{1}{2} \operatorname{erfc}[(x_0 - bt)/\sqrt{4t}] , \tag{10a}$$

$$N_1(t|x_0) = \tfrac{1}{2} \exp(bx_0) \operatorname{erfc}[(x_0 + bt)/\sqrt{4t}] , \tag{10b}$$

$$N_2(t|x_0) = 1 - N_0(t|x_0) - N_1(t|x_0) . \tag{10c}$$

The physical interpretation of these probabilities will motivate an algorithm for random displacements that reproduces Eq. (5). For this purpose we consider the rate at which particles collide with the boundary for the first time, given by

$$\nu(t|x_0) = \frac{x_0}{\sqrt{4\pi t^3}} \exp[-(x_0 - bt)^2/4t] . \tag{11}$$

One can express $p_1(x, t|x_0)$ in terms of the rate $\nu(t|x_0)$ and $p_0(x, t|x_0)$, the outgoing collision-free distribution starting at the boundary

$$p_1(x, t|x_0) = \int_0^t d\tau\, p_0(x, t - \tau|0)\, \nu(\tau|x_0) . \tag{12}$$

The interpretation of this result is the following: $p_0(x, t|x_0)$ describes those particles which appear not to have hit the boundary during time t, $p_1(x, t|x_0)$ describes particles which appear to have hit the boundary once in time t; the remaining particles are described by $p_2(x, t|x_0)$. To mimic the diffusion process our algorithm will distinguish between these three possibilities, i.e., it will reproduce the partial distribution (6)–(8).

The algorithm suggested will distribute particles in a *first step* according to the Gaussian process (6). It may happen, however, that some particles thus distributed lie *behind* the boundary. In this case the algorithm should simulate distribution (12). Since the algorithm reproduces only the *outcome* of a diffusion process after time t without knowledge of *intermediate* diffusive motion, the actual arrival times and, hence, the arrival rate $\nu(\tau|x_0)$ are not known. To obtain arrival times at the boundary, an *ad hoc* assumption about the intermediate diffusive motion must be introduced. The assumption made is that intermediate diffusion trajectories are determined by the local drift velocity $\beta F(x)$ superimposed on a *constant* random velocity. This provides an arrival time τ at the boundary (see Appendix A) for which the corresponding distribution of times is

$$\dot{n}(\tau|x_0) = [x_0^2 t/(4\pi\tau^4)]^{1/2} \exp[-(x_0 - b)^2 t/4\tau^2] . \tag{13}$$

In analogy to Eq. (12) this rate suggests the approximation

$$p_1(x, t|x_0) \approx 2 \int_0^t d\tau\, p_0(x, t - \tau|0)\, \dot{n}(\tau|x_0), \quad x \geq -b(t - \tau) . \tag{14}$$

Thus, in a *second step*, the algorithm distributes particles according to the Gaussian process $p_0(x, t - \tau|0)$. If particles end up again behind the boundary, they are distributed in a *third step* according to expression (8) approximated by a Boltzmann distribution. For a constant force this implies the approximation

$$p_2(x, t|x_0) \approx \begin{cases} 2b \exp(-bx) \displaystyle\int_0^t d\tau \int_{-b(t-\tau)}^0 dx'\, p_0(x', t - \tau|0)\, \dot{n}(\tau|x_0), & b > 0, \\ 0, & b \leq 0 . \end{cases} \tag{15}$$

The factor 2 included in Eqs. (14) and (15) assures that the sum of the two distributions produces the correct fraction $N_1(t|x_0) + N_2(t|x_0)$ of events.

Certainly other algorithms could be suggested. For example, an algorithm might first partition events corresponding to fractions $N_i(t|x_0)$ and then reproduce the corresponding distributions (6), (7), and (8). However, our suggestion, which is based solely on the boundary-free diffusion distribution and the Boltzmann distribution, can be directly generalized to linear force diffusion. We will now explicitly show how diffusive behavior governed by distribution (6) and the approximate distributions (14) and (15) can be computer simulated by use of a conventional random number generator.

The starting point for a diffusion step of time t is x_0, say. The algorithm randomly chooses endpoints x to approximately conform to distribution (5). For diffusion in the absence of boundaries and in a constant force the procedure is standard. A random number r is generated on the interval $[0, 1]$[10] and the jump endpoint is found by inverting the cumulative distribution function,[11] i.e., by solving

$$r = \int_{-\infty}^{x} dy\, p_0(y, t|x_0) \tag{16}$$

for x. One obtains

$$x = x_0 - bt + \sqrt{4t}\, \operatorname{erfc}^{-1}(2r) , \tag{17}$$

where $\operatorname{erfc}^{-1}(z)$ denotes the inverse complementary error

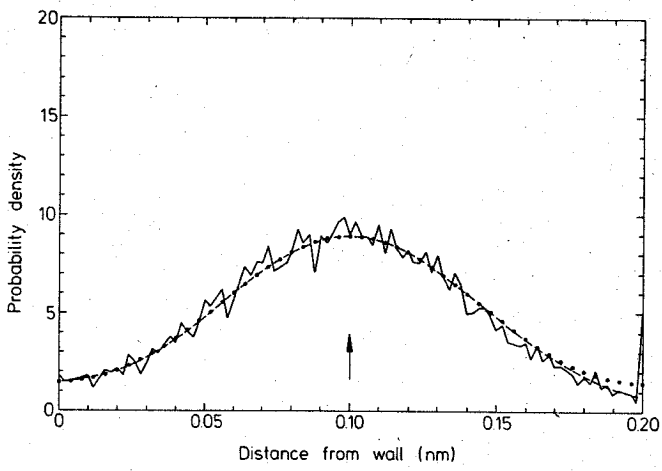

FIG. 1. Results for the probability distribution $p(x,\ t=0.001\ \text{nm}^2 \mid x_0=0.1\ \text{nm})$ for *free diffusion* near a reflective boundary (at $x=0$) as described by the Brownian dynamics algorithm of Sec. II averaging over 10^4 trials (——), by the analytical expression of Eq. (27) (- - -), and by the numerical solution of Appendix C (• • •). The arrow indicates the starting position $x_0=0.1$ nm; the numerical solution assumed an artificial reflective boundary at 0.2 nm; all particles found at $x>0.2$ nm in the Brownian dynamics method are collected in the last partition at $x=0.2$ nm.

function.[9] For a linear force (see Appendix C for the corresponding diffusion equation)

$$-\beta F(x)=b+cx\ . \tag{18}$$

The distribution $p_0(x,t\mid x_0)$ describes the Ornstein–Uhlenbeck[12] process $[\theta=1-\exp(-2ct)]$,

$$p_0(x,t\mid x_0)=[c/2\pi\theta]^{1/2}\exp\{-c[x+(b/c)\times(x_0+b/c)\exp(-ct)]^2/2\theta\} \tag{19}$$

leading to the jump endpoint

$$x=x_0\exp(-ct)-(b/c)[1-\exp(-ct)]+\{(2/c)[1-\exp(-2ct)]\}^{1/2}\ \text{erfc}^{-1}(2r)\ . \tag{20}$$

For x_0 chosen close to the boundary, a significant number of trajectories will have endpoints beyond the boundary ($x<0$). A corresponding particle has diffused to the boundary and hit at least once. For free diffusion ($b=c=0$) only $p_1(x,t\mid x_0)$ in Eq. (5) contributes to the reflected contribution. In this case the total distribution is reproduced by the following modification of Eq. (17):

$$x=\left|x_0+\sqrt{4t}\ \text{erfc}^{-1}(2r)\right|\ , \tag{21}$$

i.e., by reflecting the endpoint back onto the positive x axis. It has been shown[6] that this procedure reproduces the diffusion distribution exactly (within statistical error).

The generalization of Eq. (21) in the presence of a force requires one to determine the time τ_B when a particle with $x<0$ has arrived at the boundary. This arrival time is (Appendix A)

$$\tau_B=\frac{1}{c}\ln\left(\frac{x_0-x}{x_0e^{-ct}-x}\right), \tag{22}$$

which in the case of a constant force ($c=0$) reduces to

$$\tau_B=x_0t/(x_0-x)\ . \tag{23}$$

The jump endpoint is then determined by assuming a diffusion step away from the boundary covering the remaining time period $t-\tau_B$. For this purpose a second random number r' is chosen which yields ($t'=t-\tau_B$)

$$x'=x_0\exp(-ct')-(b/c)[1-\exp(-ct')]+\{(2/c)[1-\exp(-2ct')]\}^{1/2}\left|\text{erfc}^{-1}(2r')\right| \tag{24}$$

or, for $c=0$,

$$x'=x_0-bt'+\sqrt{4t'}\left|\text{erfc}^{-1}(2r')\right|\ . \tag{25}$$

The absolute value of $\text{erfc}^{-1}(2r')$ in these expressions accounts for the condition that the random contribution to the displacement is directed *away* from the boundary.

For forces attractive toward the boundary it is possible that the jump endpoint x resulting from Eq. (24) or (25) is again negative. This corresponds to the occurrence of secondary, tertiary, etc., encounters with the boundary. In this case a third random number r'' is chosen and the particle finally distributed according to

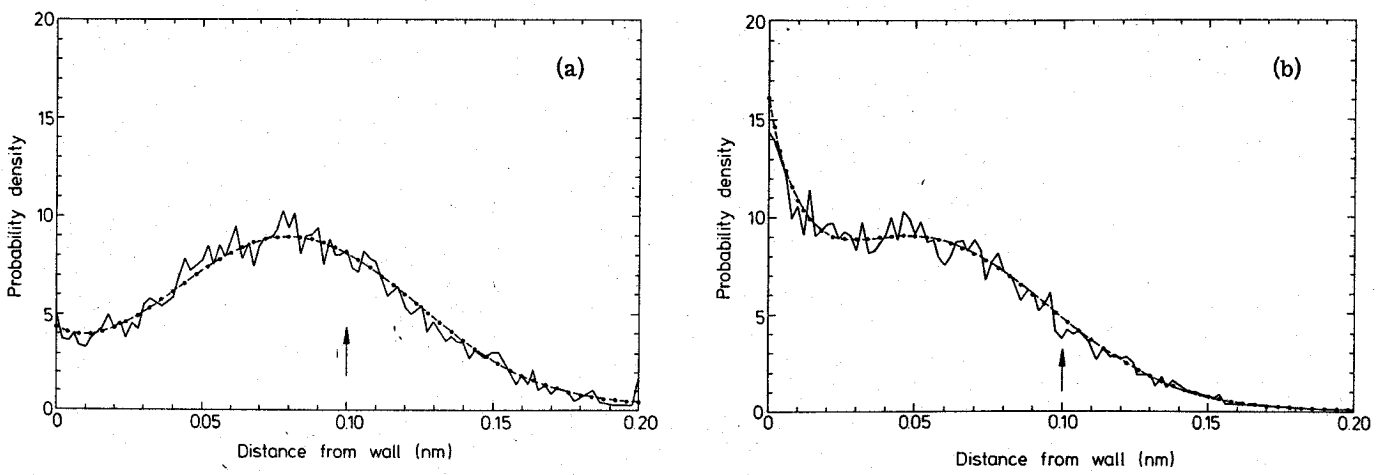

FIG. 2. (a) Results for the probability distribution $p(x,\ t=0.001\ \text{nm}^2 \mid x_0=0.1\ \text{nm})$ for *diffusion in the constant force* $\beta F(x)=-20\ \text{nm}^{-1}$ near a reflective boundary (at $x=0$). For further details refer to the caption for Fig. 1. (b) Results for the probability distribution $p(x,\ t=0.001\ \text{nm}^2 \mid x_0=0.1\ \text{nm})$ for *diffusion in the constant force* $\beta F(x)=-50\ \text{nm}^{-1}$ near a reflective boundary (at $x=0$). For further details refer to the caption for Fig. 1.

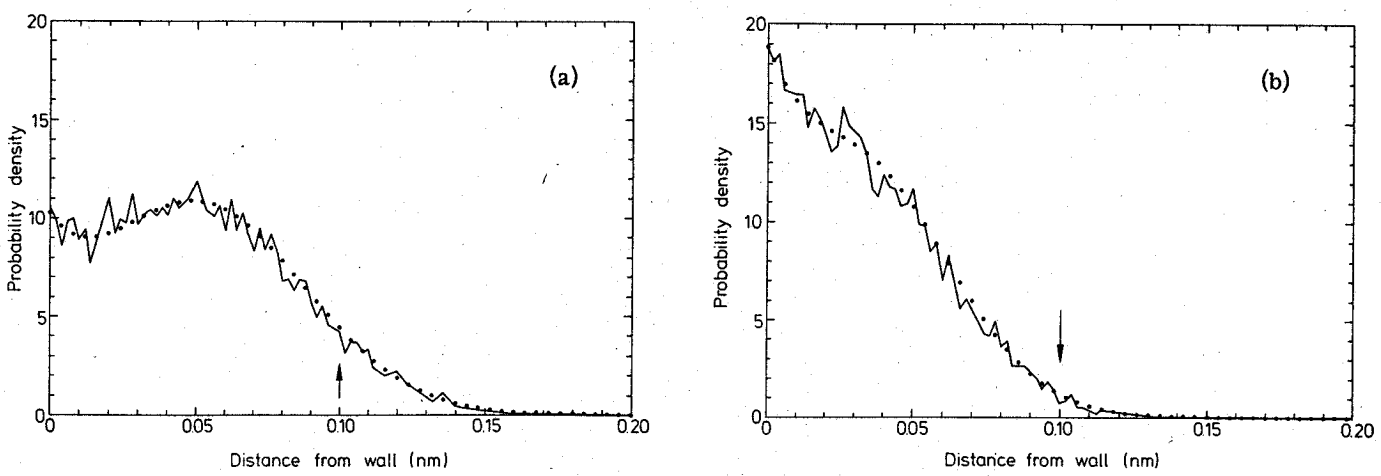

FIG. 3. (a) Results for the probability distribution $p(x,\ t=0.001\ \text{nm}^2\,|\,x_0=0.1\ \text{nm})$ for *diffusion in the linear force* $\beta F(x)=(-20-200\,x)\ \text{nm}^{-1}$ near a reflective boundary (at $x=0$). For further details refer to the caption for Fig. 1. (b) Results for the probability distribution $p(x,\ t=0.001\ \text{nm}^2\,|\,x_0=0.1\ \text{nm})$ for *diffusion in the linear force* $\beta F(x)=(-20-400\,x)\ \text{nm}^{-1}$ near a reflective boundary (at $x=0$). For further details refer to the caption for Fig. 1.

$$r'' = \frac{1}{N}\int_0^{x''} dy\, p_2(y, t-\tau_B\,|\,0)\ , \tag{26}$$

where $N=\int_0^\infty dy\, p_2(y, t-\tau_B\,|\,0)$. The inversion of this expression to yield x'' is discussed in Appendix B. It is sufficient to say here that for attractive forces $p_2(y, t-\tau_B\,|\,0)$ resembles the Boltzmann distribution. Hence, the algorithm reproduces the trend toward a Boltzmann distribution of particles caught in a potential well near a reflective boundary.

III. TEST OF THE ALGORITHM

In this section we demonstrate the validity of the algorithm for diffusive displacements in a linear force near a reflective boundary. For this purpose the outcome of 10^4 random choices of endpoints x is monitored and compared with probability distributions evaluated by conventional methods, viz., analytical solutions available for the constant force situation and finite-difference solutions (Appendix C) of the Einstein–Smoluchowski diffusion equation.

For our calculations we chose an initial position $x_0=0.1$ nm near the boundary (at $x=0$) and assumed a time duration of $t=10^{-3}$ nm^2 corresponding to a diffusive broadening of about 0.06 nm. Force constants were chosen to yield illustrative examples. The diffusion space $0<x<0.2$ nm was partitioned into 100 intervals of equal width. The number of random endpoints in each partition was recorded and the distribution normalized after 10^4 applications of the algorithm (10^5 for Fig. 4), which took about 3 sec CPU time on a Univac 1182 installation. Endpoints beyond $x=0.2$ nm were collected in the last partition to provide a measure of the number of particles escaped from the diffusion space. A diffusion space of $0<x<0.2$ nm with 100 partitions was also used in the finite-difference solution. In the following Figs. 1–6, the results are shown only for every other partition.

Figure 1 presents results for free diffusion ($b=c=0$). The Brownian dynamics algorithm reproduces well the analytical solution

$$(4\pi t)^{-1/2}\{\exp[-(x-x_0)^2/4t]+\exp[-(x+x_0)^2/4t]\}\ . \tag{27}$$

The finite-difference method also yields good results except near $x=0.2$ nm, where a reflective boundary has been assumed.

Diffusion in a constant force is illustrated in Figs. 2a and 2b for $b=20\ \text{nm}^{-1}$ and $b=50\ \text{nm}^{-1}$, respectively. The main features in comparison to the free diffusion situation in Fig. 1 is the drift of the probability maximum by $-bt$ and the appearance of a Boltzmann-like distribution near the boundary. All three descriptions, analytical, numerical and Brownian dynamics, are in agreement. However, for the stronger force the Brownian dynamics method slightly underestimates the probability density at the boundary. Based on additional data for forces up to $b=700\ \text{nm}^{-1}$, a 10% underestimate seems to be a systematic error due to the approximations involved in accounting for the $p_2(x, t\,|\,x_0)$ contribution. The error can be attributed in part to neglect of

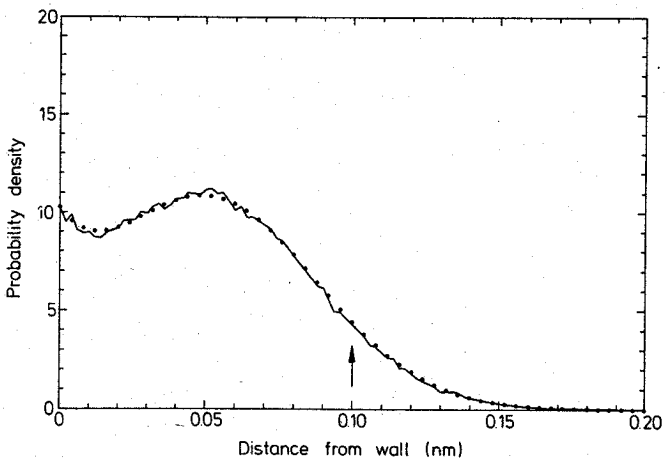

FIG. 4. Results for the probability distribution $p(x,\ t=0.001\ \text{nm}^2\,|\,x_0=0.1\ \text{nm})$ for *diffusion in the linear force* $\beta F(x)=(-20-200\,x)\ \text{nm}^{-1}$ near a reflective boundary (at $x=0$) averaging over 10^5 (rather than 10^4) trials of the Brownian dynamics method. For further details refer to the caption for Fig. 1.

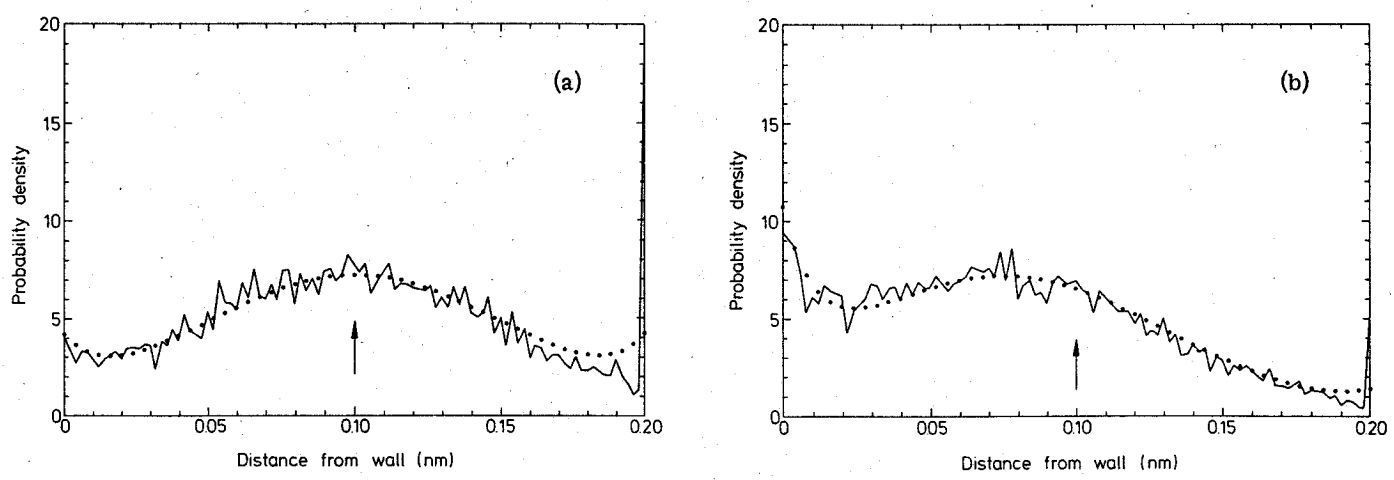

FIG. 5. (a) Results for the probability distribution $p(x, t=0.001\ \text{nm}^2 \mid x_0=0.1\ \text{nm})$ for *diffusion in the linear force* $\beta F(x)=(-40+200\,x)\ \text{nm}^{-1}$ near a reflective boundary (at $x=0$). For further details refer to the caption for Fig. 1. (b) Results for the probability distribution $p(x, t=0.001\ \text{nm}^2 \mid x_0=0.1\ \text{nm})$ for *diffusion in the linear force* $\beta F(x)=(-60+200\,x)\ \text{nm}^{-1}$. For further details refer to the caption for Fig. 1.

the erfc(x) factor of $p_2(x, t \mid x_0)$ [see Eq. (8) and Appendix B].

In Figs. 3a and 3b we present the probability distribution for two different linear forces with negative slopes superimposed on the constant force of Fig. 2a. A comparison with Fig. 2a shows clearly the further drift of particles toward the boundary. As an analytical solution is not available for the linear force case, only results of the finite-difference and the Brownian dynamics methods are compared. The agreement between the two methods is good. The scatter in the Brownian dynamics results, is of course, of statistical origin and can be reduced if the number of trials is increased. This is demonstrated in Fig. 4 which shows the result of 10^5 (rather than 10^4) applications of the Brownian dynamics method, thereby decreasing the scatter by a factor of about $10^{-1/2}$.

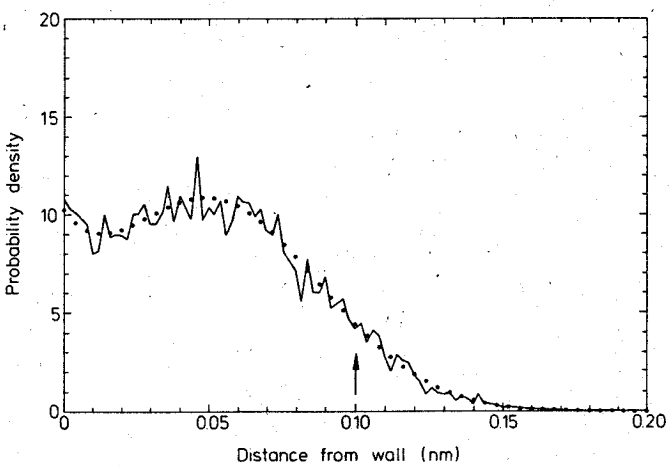

FIG. 6. Results for the probability distribution $p(x, t=0.001\ \text{nm}^2 \mid x_0=0.1\ \text{nm})$ for *diffusion in the linear force* $\beta F(x)=(-20-200\,x)\ \text{nm}^{-1}$ near a reflective boundary (at $x=0$) comprising the Brownian dynamics distribution of 100-jump trajectories (with each displacement of $10^{-5}\ \text{nm}^2$ time duration) rather than of single displacements (of $10^{-3}\ \text{nm}^2$ time duration). For further details refer to the caption for Fig. 1.

Figs. 5a and 5b represent diffusion in a linear force with positive slopes superimposed on a constant force. Figure 5a corresponds to the situation that the diffusing particle is initially located at the point of zero force (potential maximum). The broad Gaussian spread and the absence of two relative maxima of the distribution agree with remarks by van Kampen[13] on diffusion in a quadratic potential. The effect of the wall is slight but noticeable in the asymmetry of the Brownian dynamics result (the finite difference result is symmetrical because of the artificial reflective boundary at 0.2 nm). The potential maximum corresponding to the force of Fig. 5b occurs at $x=0.15$ nm, i.e., the diffusing particle is initially situated on a slope attractive toward the boundary. The expected drift and the development of Boltzmann character near the boundary is clearly shown. There is also significant diffusion over the barrier with 10% of the particles escaping.

Finally, the question arises whether the outcome of the simulation of diffusion trajectories by the extended Brownian dynamics algorithm devised here depends on the choice of jump times. For an answer we have repeated our calculations for diffusion in the linear force of Fig. 3a, but comprising the distribution of 100-jump trajectories (with each displacement of $10^{-5}\ \text{nm}^2$ time duration) rather than single displacements (of $10^{-3}\ \text{nm}^2$ time duration). The results presented in Fig. 6 again closely agree with the results of the finite-difference method, except for a slight increase in scatter. Thus the simulation by the extended Brownian dynamics algorithm is invariant of the jump times chosen, and in an actual application one can choose jump times as long as can be reconciled with the local approximation of the actual force by a linear field and with the shape of the boundaries.

ACKNOWLEDGMENTS

The authors are grateful to Dr. Z. Schulten for very helpful suggestions concerning the numerical part of this work. The use of the computer facilities of the Gesellschaft für Wissenschaftliche Datenverarbeitung, Göttingen is acknowledged.

APPENDIX A: EVALUATION OF THE TIME OF ARRIVAL τ_B

We determine here the time of arrival at a boundary at $X=0$ for a diffusion step of duration t described by the path $X(\tau)$ which carries a particle from $X(\tau=0)=x_0>0$ to $X(\tau=t)=x<0$. The path $X(\tau)$ obeys the Langevin equation

$$\dot{X}=m\beta A(\tau)+\beta F(X)\,, \tag{A1}$$

where m is the particle mass, $A(\tau)$ the stochastic force due to the bath and $F(X)$ the external force. The algorithm adopted in Sec. II for the diffusive displacements corresponds to the representation of the stochastic term in (A1) by a *constant* (random) velocity, viz.,

$$m\beta A(\tau)=v_r\,, \tag{A2}$$

which complies with the initial and final position. For a linear force we have then

$$\dot{X}=v_r-b-cX\,. \tag{A3}$$

We like to determine the time of arrival at the boundary τ_B which is defined by the equation

$$X(\tau_B)=0\,. \tag{A4}$$

For this purpose we note that the solution of Eq. (A3) is

$$X(\tau)=x_0\,e^{-c\tau}-\frac{(x_0\,e^{-ct}-x)(1-e^{-c\tau})}{(1-e^{-ct})}\,, \tag{A5}$$

which yields

$$\tau_B=c^{-1}\ln[(x_0-x)/(x_0\,e^{-ct}-x)]\,. \tag{A6}$$

For a constant force, i.e. $c=0$, these solutions simplify to

$$X(\tau)=x_0-\frac{(x_0-x)\tau}{t} \tag{A7}$$

and

$$\tau_B=x_0\,t/(x_0-x)\,. \tag{A8}$$

APPENDIX B: EVALUATION OF ENDPOINTS x'' FROM $p_2(x,t|0)$

The integral for the jump endpoint x'' given by

$$r=\int_0^{x''}dy\,p_2(y,t-\tau_B|0)\,, \tag{B1}$$

where

$$p_2(x,t|0)=\tfrac{1}{2}b\,\frac{\exp(-bx)\operatorname{erfc}[(x-bt)/\sqrt{4t}\,]}{[1-\operatorname{erfc}(b\sqrt{t}/2)]} \tag{B2}$$

cannot be inverted analytically. For bt large (and positive[14]) this expression reduces to the Boltzmann distribution

$$p_2(x,t|0)\approx b\,e^{-bx} \tag{B3}$$

and Eq. (B1) yields

$$x''=-\ln(r)/b\,. \tag{B4}$$

If b is small, the contribution of $p_2(x,t|x_0)$ to $p(x,t|x_0)$ in Eq. (5) will also be small and the approximation of little consequence. If b is large but t small, then the error can be significant. This will occur for a strong constant force and will affect those particles whose endpoints are chosen according to Eq. (B1) and where $t\sim\tau_B$. The neglect of any short-time dependence of $p_2(x,t|0)$ will tend to distribute some particles too far away from the boundary. We have found that in a strong force, approximation (B3) tends to underestimate the distribution at the boundary by about 10%. Though other approximations could be tried and Eq. (B3) possibly improved, we have used approximation (B3) in our calculations for constant forces. For a linear force one must distinguish between situations of positive and negative slopes. For positive slope, the distribution corresponding to Eq. (B3) is

$$p_2(x,t|0)\approx\sqrt{2c/\pi}\,\exp[-(c/2)(x+b/c)^2]/\operatorname{erfc}(b\sqrt{2c}) \tag{B5}$$

and Eq. (B1) yields

$$x''=-b/c+\sqrt{2/c}\,\operatorname{erfc}^{-1}[r\operatorname{erfc}(b/\sqrt{2c})],\quad c>0\,. \tag{B6}$$

For negative c the Boltzmann distribution is unbounded and hence unnormalizable. We have obtained good results using instead the distribution

$$p_2(x,t|0)\approx\begin{cases} b\,e^{-bx}/(1-e^{-b^2/|c|}), & 0\le x\le\left|\dfrac{b}{c}\right| \\ 0\,, & x>\left|\dfrac{b}{c}\right| \end{cases} \tag{B7}$$

which yields the endpoint

$$x''=-(1/b)\ln(1-r+r\,e^{-b^2/|c|})\,,\quad c<0. \tag{B8}$$

Again other approximations are possible. If a linear force approximates the actual force over short distances only, it may be suitable to construct a table of numerically generated endpoints corresponding to the actual Boltzmann distribution prior to trajectory calculations.

APPENDIX C: FINITE-DIFFERENCE SOLUTION

Here we briefly describe the solution to the one-dimensional Einstein–Smoluchowski diffusion equation for a linear force by means of the differential–difference method applied to the three-dimensional case in Ref. 1. To solve the partial differential equation

$$\frac{\partial}{\partial t}p(x,t|x_0)=\frac{\partial}{\partial x}\left[\frac{\partial}{\partial x}+(b+cx)\right]p(x,t|x_0) \tag{C1}$$

subject to

$$p(x,t=0|x_0)=\delta(x-x_0)\,, \tag{C2}$$

we discretize the spatial operator

$$\mathbf{L}(x)=\frac{\partial}{\partial x}\left[\frac{\partial}{\partial x}+(b+cx)\right] \tag{C3}$$

on the interval $[0,x_M]$. Subdividing this interval into N equal length (Δ) partitions with endpoints

$$x_j=(j-1)\Delta,\quad 1\le j\le N+1\,, \tag{C4}$$

the operator $\mathbf{L}(x)$ acting on $p(x,t|x_0)$ is represented by the tridiagonal matrix

$$L_{jj}=c-\frac{2}{\Delta^2}\,,$$

$$L_{jj\pm1}=\frac{1}{\Delta^2}\pm\frac{b}{2\Delta}\pm\frac{c(j-1)}{2},\quad 2\le j\le N\,. \tag{C5}$$

(If the force is only piecewise linear, then b and c will depend on j.) The corner elements of **L** are found by using the reflective boundary condition at $x=0$ and $x=x_M$.[15] For trapezoidal weights

$$W_1 = W_{N+1} = \tfrac{1}{2}\,, \qquad W_j = 1, \quad 2 \le j \le N\,, \tag{C6}$$

one obtains

$$L_{11} = -\frac{2}{\Delta^2} + \frac{b}{\Delta} + c, \quad L_{12} = \frac{2}{\Delta^2} + \frac{b}{\Delta}\,,$$
$$L_{N+1,N} = \frac{2}{\Delta^2} - \frac{b}{\Delta} - cN, \quad L_{N+1,N+1} = -\frac{2}{\Delta^2} - \frac{b}{\Delta} - c(N-1)\,. \tag{C7}$$

The solution to Eq. (C1),

$$p(x_j, t|x_0) = \sum_i [\exp(Lt)]_{ji}\, p(x_i, t=0|x_0) \tag{C8}$$

can be expanded in terms of eigenvectors. To diagonalize **L** one first transforms **L** to a symmetric matrix **A** through a similarity transformation

$$A_{il} = S^{-1}_{ij} L_{jk} S_{kl} = A_{li}\,, \tag{C9}$$

where

$$S_{ij} = \sigma_i \delta_{ij}\,, \tag{C10}$$

with δ_{ij} denoting the Kronecker delta and

$$\sigma_1 = 1\,, \qquad \sigma_i = \sigma_{i-1}\sqrt{L_{i,i-1}/L_{i-1,i}}\,, \quad 2 \le i \le N+1\,. \tag{C11}$$

A can be diagonalized by a unitary matrix **U**

$$U^{-1}_{ij} A_{jk} U_{kl} = \lambda_i \delta_{il}\,, \tag{C12}$$

where λ_i are the eigenvalues. Since **A** is tridiagonal, the eigenvalues λ_i and the matrix **U** were obtained by the implicit QL method.[16] In terms of **S**, **U**, and the λ_i, the solution (C8) to the Smoluchowski equation is

$$p(x_i, t|x_0) = \sigma_i \sum_{j=1}^{N+1} \frac{p(x_j, t=0|x_0)}{\sigma_j} \left[\sum_{n=1}^{N+1} U_{in}(\lambda_n t) U_{jn}\right]. \tag{C13}$$

The initial condition in the discretized representation is

$$p(x_j,\ t=0|x_0) = \frac{\delta_{jJ}}{W_J \Delta}\,, \tag{C14}$$

where $J = \mathrm{Int}(Nx_0/x_M) + 1$, $\mathrm{Int}(x)$ denoting the integer *closest* to x. Combination of Eqs. (C13) and (C14) yields

$$p(x_i, t|x_0) = \frac{\sigma_i}{W_J \Delta \sigma_J} \sum_{n=1}^{N+1} U_{in} \exp(\lambda_n t) U_{Jn}\,. \tag{C15}$$

[1] See for example, Z. Schulten and K. Schulten, J. Chem. Phys. **66**, 4616 (1977).

[2] For recent work on stilbene photoisomerization see B. I. Greene, R. M. Hochstrasser, and R. B. Weisman, Chem. Phys. Lett. **62**, 427 (1979); for theoretical work on photoisomerization see J. A. Montgomery, D. Chandler, and B. J. Berne, J. Chem. Phys. **70**, 4056 (1979).

[3] K. A. Zachariasse, W. Kühnle, and A. Weller, Chem. Phys. Lett. **59**, 375 (1978).

[4] R. M. Levy, M. Karplus, and J. A. McCammon, Chem. Phys. Lett. **65**, 4 (1979).

[5] D. L. Ermak and J. A. McCammon, J. Chem. Phys. **69**, 1352 (1978).

[6] K. Schulten and I. Epstein, J. Chem. Phys. **71**, 309 (1979).

[7] D. L. Ermak, J. Chem. Phys. **62**, 4197 (1975).

[8] M. V. Smoluchowski, Phys. Z. **17**, 557, 585 (1916).

[9] M. Abramowitz and I. A. Stegun, *Handbook of Mathematical Functions* (Dover, New York, 1972), p. 297.

[10] A pseudorandom integer was generated on the interval $[0, 2^{35}]$ by the congruence method and then converted to a random number r on the interval [0, 1]. For a discussion of pseudorandom numbers, see Ref. 11.

[11] J. M. Hammersley and D. C. Handscomb, *Monte Carlo Methods* (Wiley, New York, 1964).

[12] G. E. Uhlenbeck and L. S. Ornstein, Phys. Rev. **36**, 823 (1930). [This paper is reprinted in *Selected Papers on Noise and Stochastic Processes*, edited by N. Wax (Dover, New York, 1954).]

[13] N. G. van Kampen, J. Stat. Phys. **17**, 71 (1977).

[14] If $b \le 0$ at $x=0$, then according to Eq. (14) the drift term assures that all end points calculated from Eq. (25) will be positive.

[15] An absorbing boundary condition at $x=x_M$ is also possible (see Ref. 1 above).

[16] B. T. Smith, J. M. Boyle, B. S. Garbow, Y. Ikebe, V. C. Ken, and G. B. Moler, *Matrix Eigensystem Routines–Eispack Guide Book*, Lecture Notes in Computer Science (Springer, New York, 1974), Vol. 6.